Supplement of Ocean Sci., 18, 693–715, 2022
https://doi.org/10.5194/os-18-693-2022-supplement

Ocean Science Open Access EGU

Supplement of

Influence of cyclonic and anticyclonic eddies on plankton in the southeastern Mediterranean Sea during late summertime

Natalia Belkin et al.

Correspondence to: Eyal Rahav (eyal.rahav@ocean.org.il) and Natalia Belkin (belkin@ocean.org.il)

Influence of cyclonic and anti-cyclonic eddies on plankton in the southeastern Mediterranean Sea during late summertime

By Belkin et al

Supplementary Material

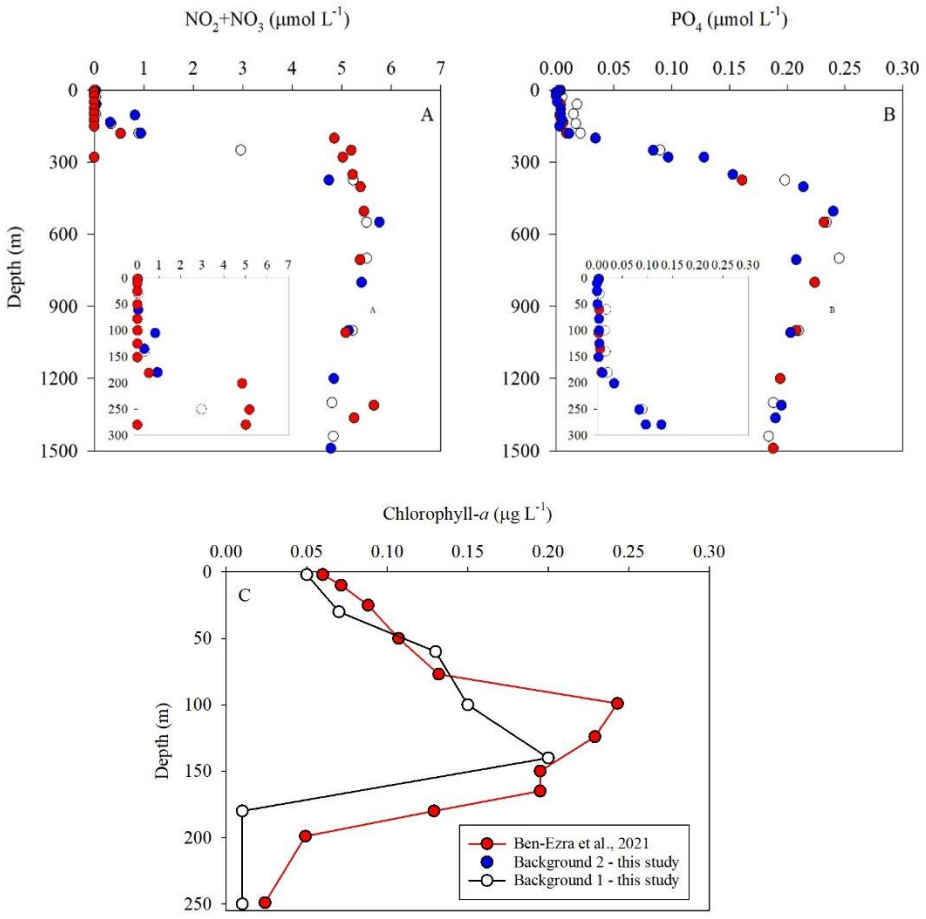

Figure S1 – Comparison between the vertical profiles of NO_2+NO_3 (A), PO_4 (B) and chlorophyll-*a* (C) at the station used as 'background' in this study (white, Lat. 32.95 N, Lon. 34.46 E); a station located between the eddies (blue, Lat. 32.66; Lon. 33.76) and an offshore station at the THEMO mooring (red, Lat. 32.82; Lon. 34.95, Ben-Ezra et al., 2021; Reich et al., 2022). All offshore stations were sampled at the same time as in our study (October 2018). Kruskal-Wallis One Way Analysis of Variance on Ranks shows the vertical profiles were insignificantly different; P=0.63, P=0.43 and P=0.24 for NO_2+NO_3, PO_4 and chlorophyll-*a*, respectively. Insert in panels A and B: the upper 300 m.

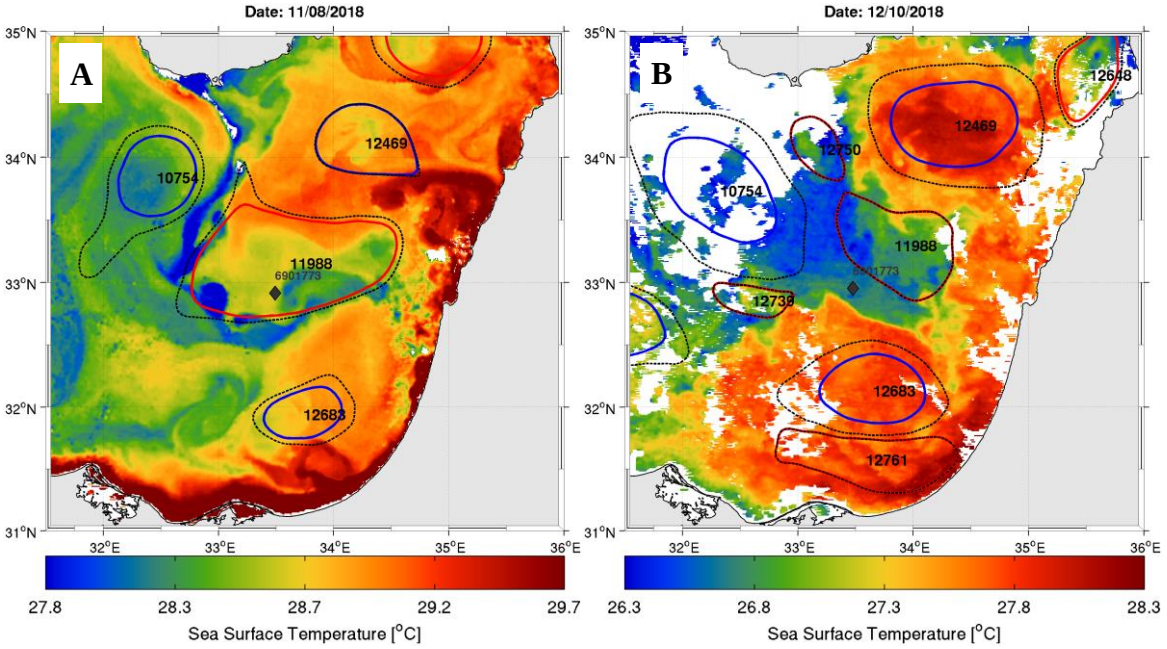

Figure S2 – Sea surface temperature maps with eddies detected by the AMEDA algorithm for 11/08/2018 (A), and 12/10/2018 (B).

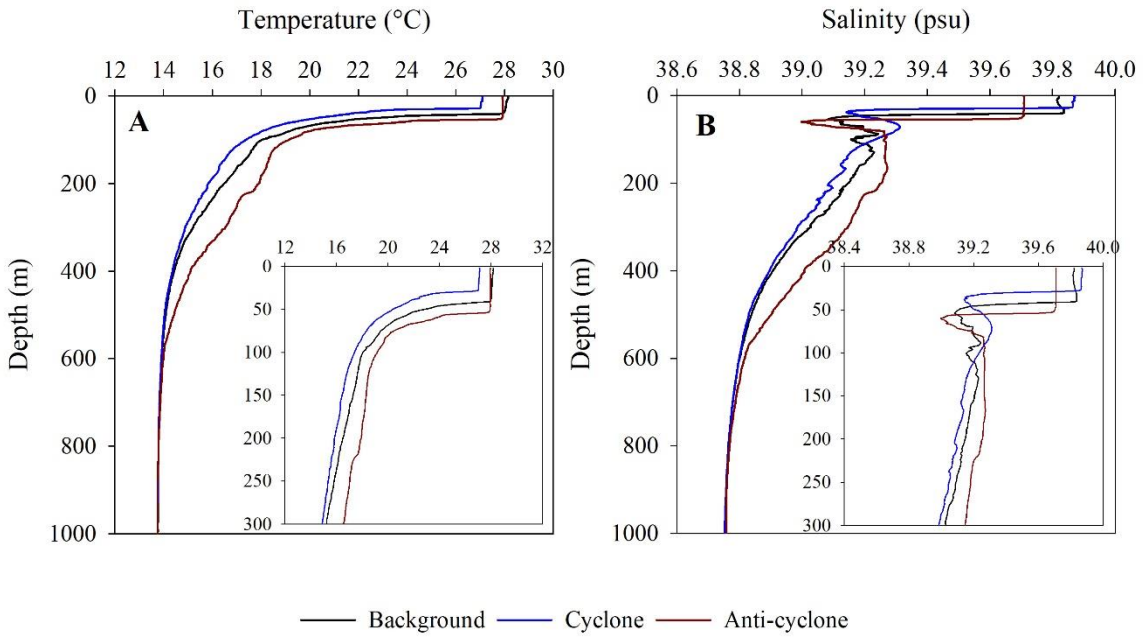

Figure S3 – Vertical profiles of temperature (A) and salinity (B) in cyclonic and anti-cyclonic eddies and an uninfluenced background station at the southeastern Mediterranean Sea. Inserts show the upper 300 m of the water column.

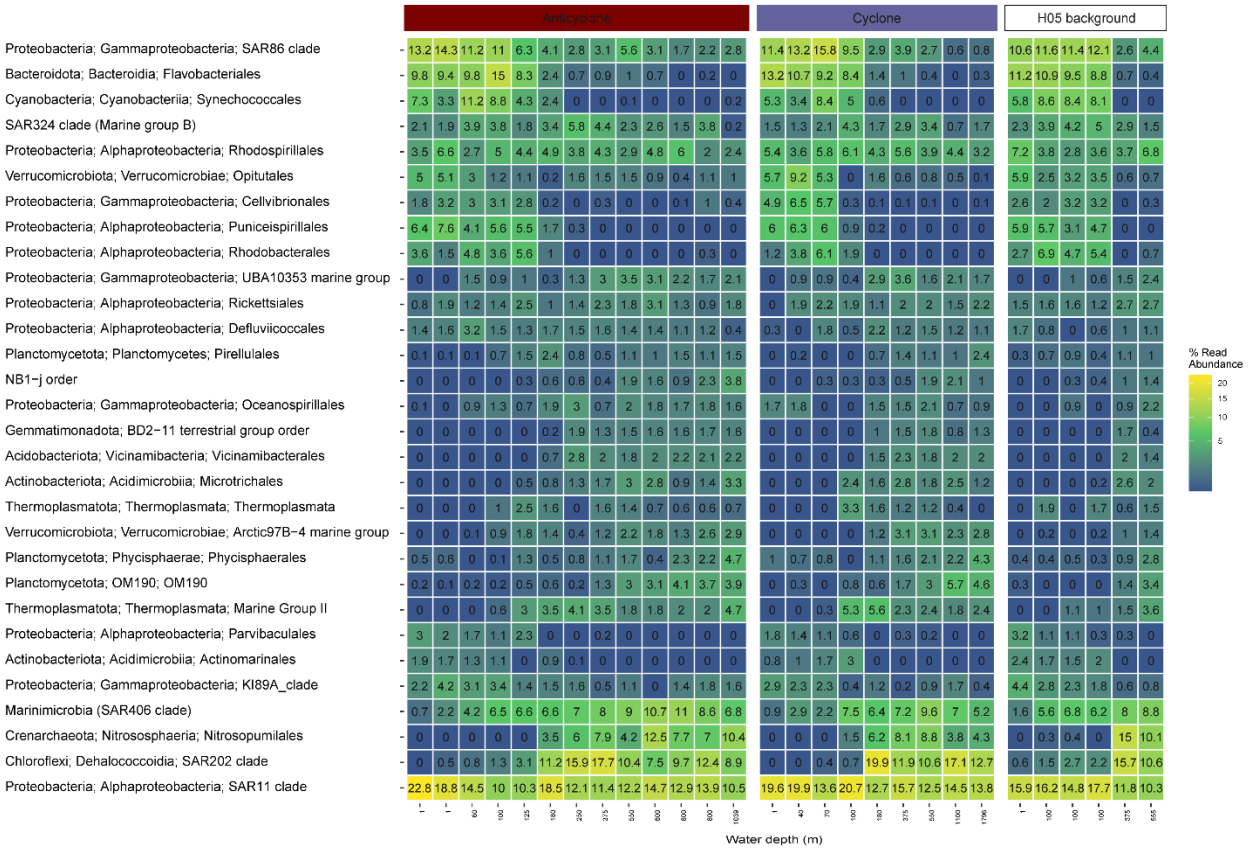

Figure S4. The relative abundance of 30 most-abundant bacterial and archaeal lineages (order level) was collected at cyclonic and anti-cyclonic eddies, and an uninfluenced background station (H05) at the southeastern Mediterranean Sea during October 2018, as estimated by read abundance. Results of replicate casts in anti-cyclone and control H05 stations are shown.

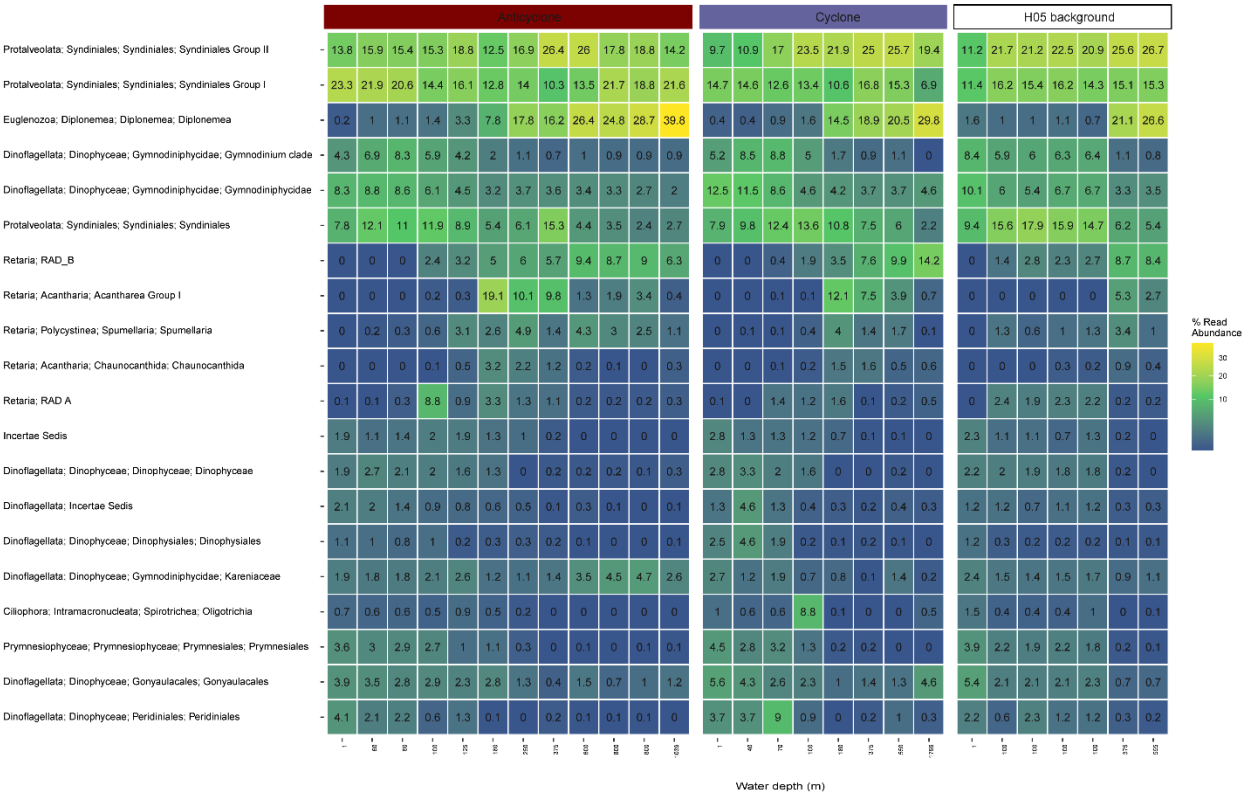

Figure S5. The relative abundance of 20 most-abundant unicellular eukaryotic lineages (taxonomy level 5 or the highest detectable level below the 5th) collected at cyclonic and anti-cyclonic eddies, and an uninfluenced background station (H05) at the southeastern Mediterranean Sea during October 2018, as estimated by read abundance. Results of replicate casts in anti-cyclone and control H05 stations are shown.

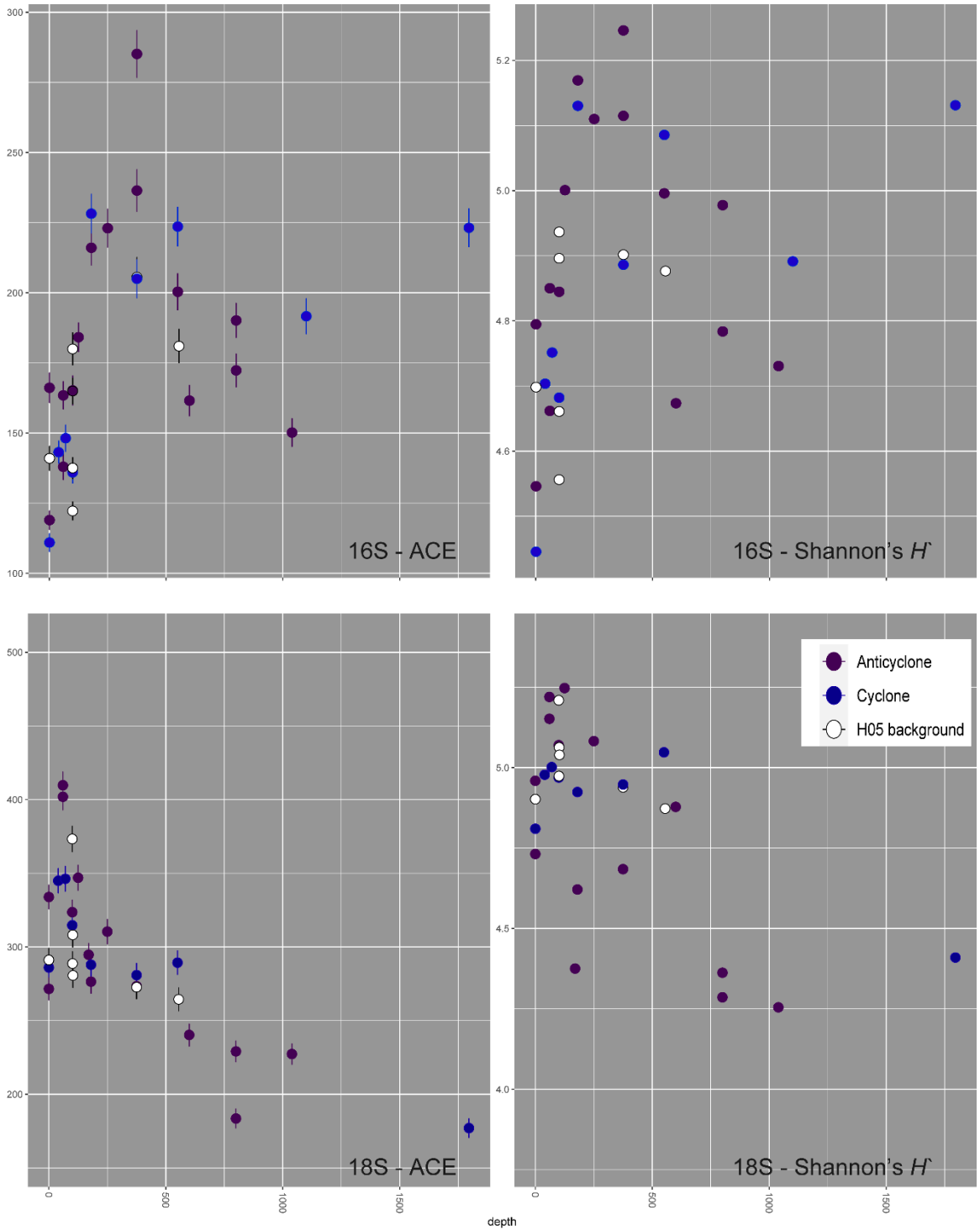

Figure S6. Species richness (as ACE) and diversity (as Shannon's *H*, log 10 base) in bacterioplankton (top) and unicellular planktonic eukaryotes (bottom) communities, estimated by amplicon sequence variant counts. Eukaryotic diversity decreases with depth, while that of bacterioplankton peaks below the deep chlorophyll maximum.

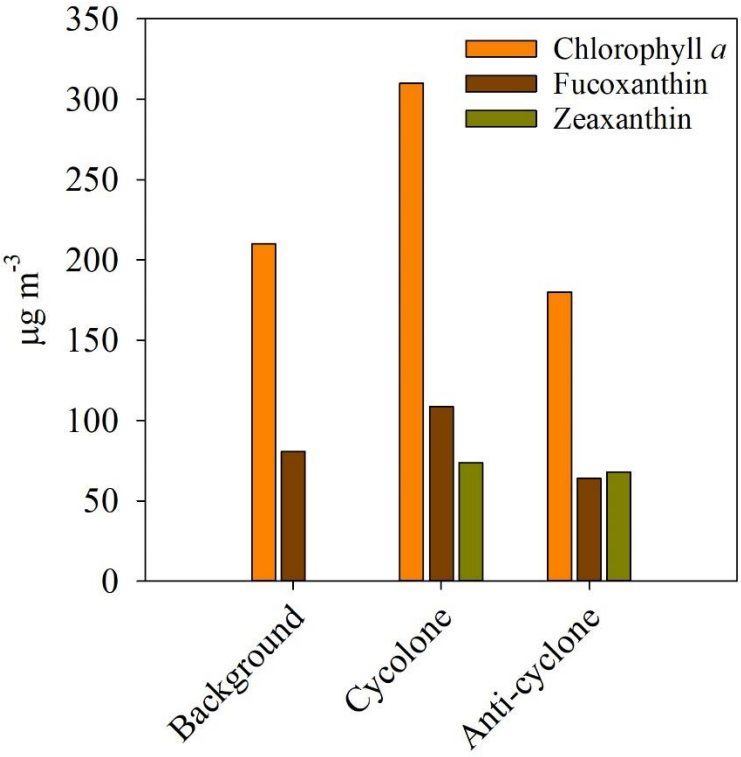

Figure S7. Main photosynthetic pigment markers that were found at the DCM at each station. Chlorophyll *a* – the main photosynthetic pigment; Fucoxanthin – auxiliary pigment of diatoms, chrysophytes and some prymnesiophytes; and Zeaxanthin – auxiliary pigment marker of green algae and cyanobacteria.

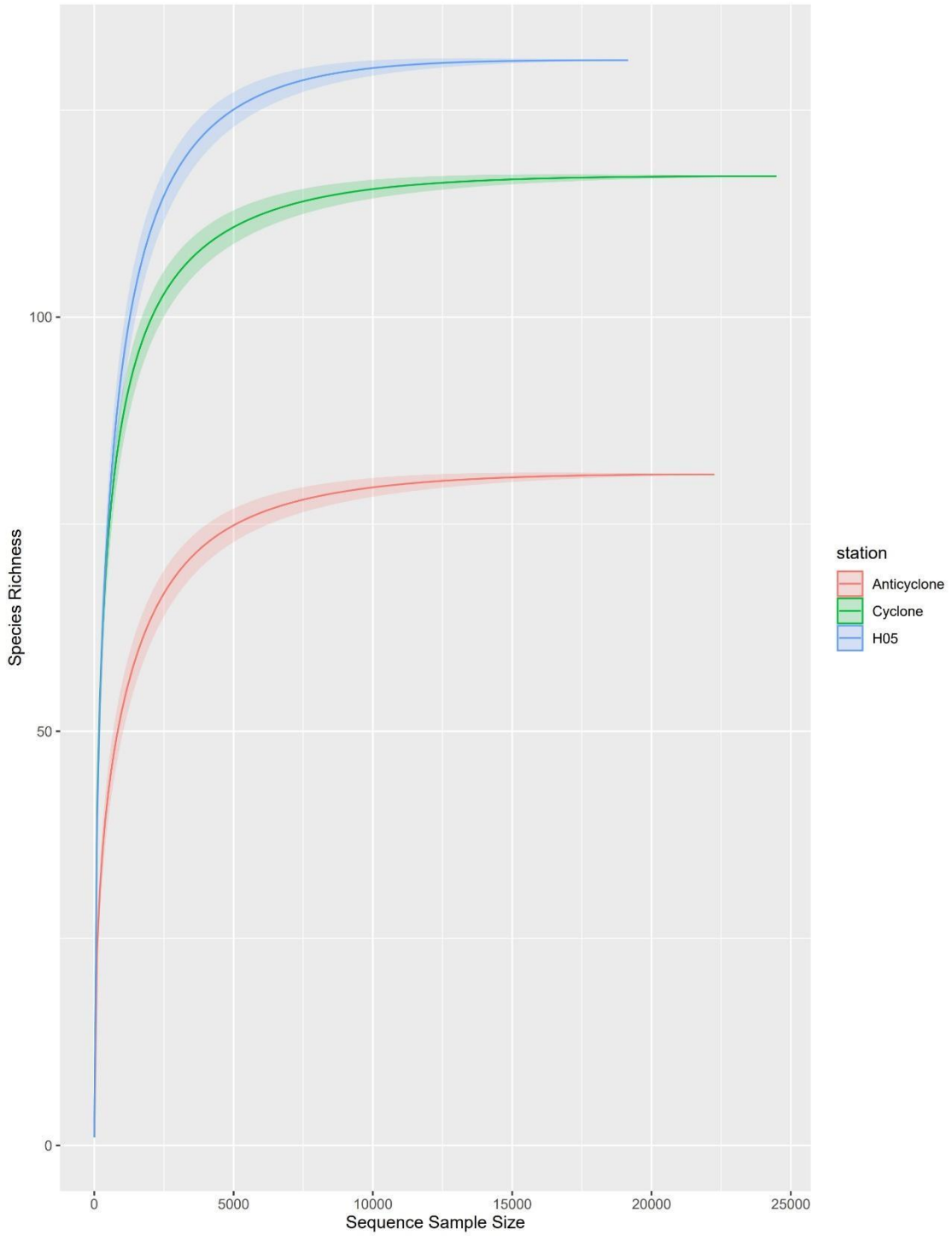

Figure S8. Rarefaction curves of observed 18S rRNA gene ASVs retrieved from 0-300m vertical net samples of mesozooplankton >100-µm collected at cyclonic and anti-cyclonic eddies and an uninfluenced background station (H05) at the Eastern Mediterranean Sea during October 2018.

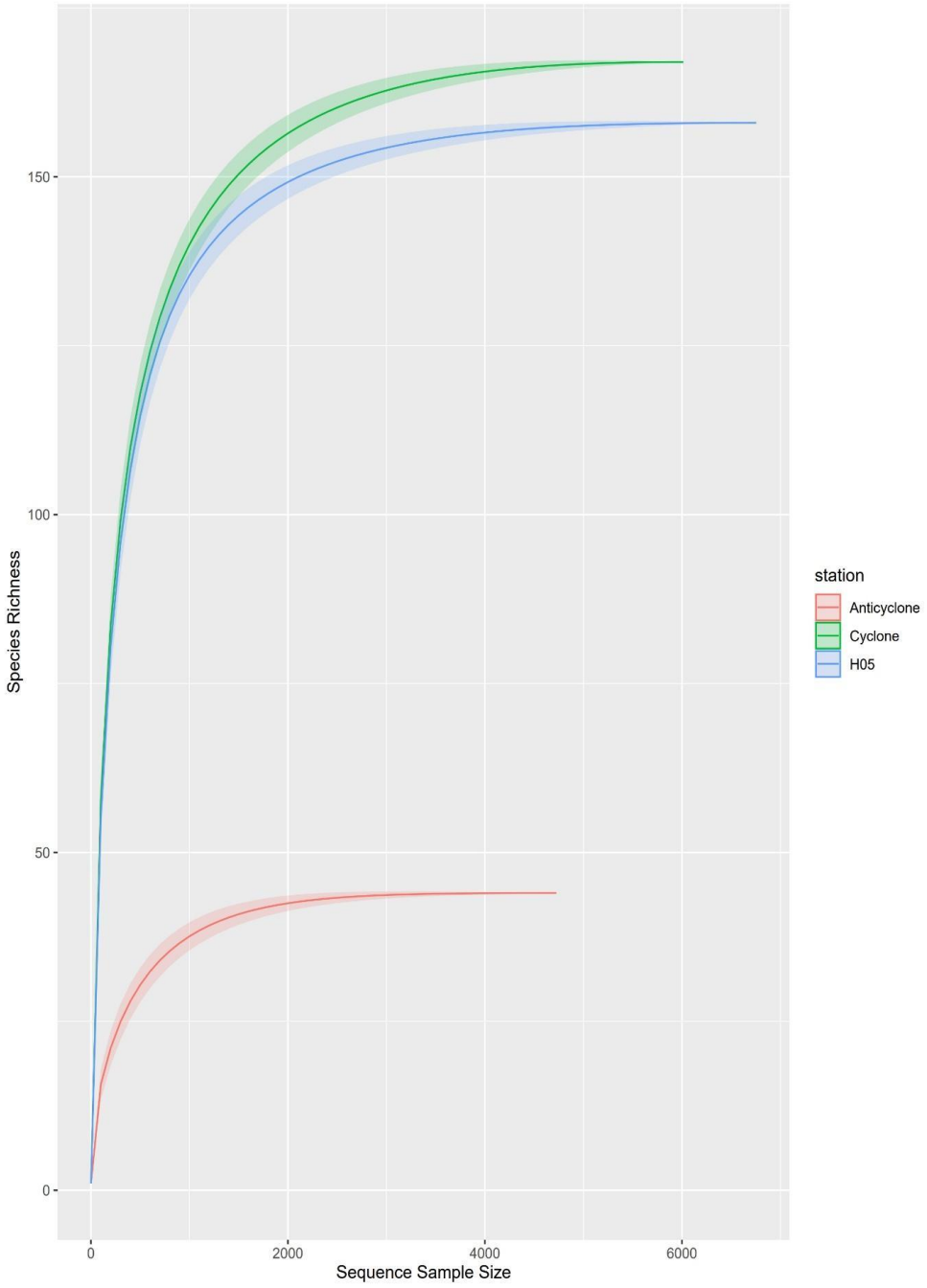

Figure S9. Rarefaction curves of observed COI gene ASVs retrieved from 0-300m vertical net samples of mesozooplankton >100-µm collected at cyclonic and anti-cyclonic eddies, and an uninfluenced background station (H05) at the Eastern Mediterranean Sea during October 2018.

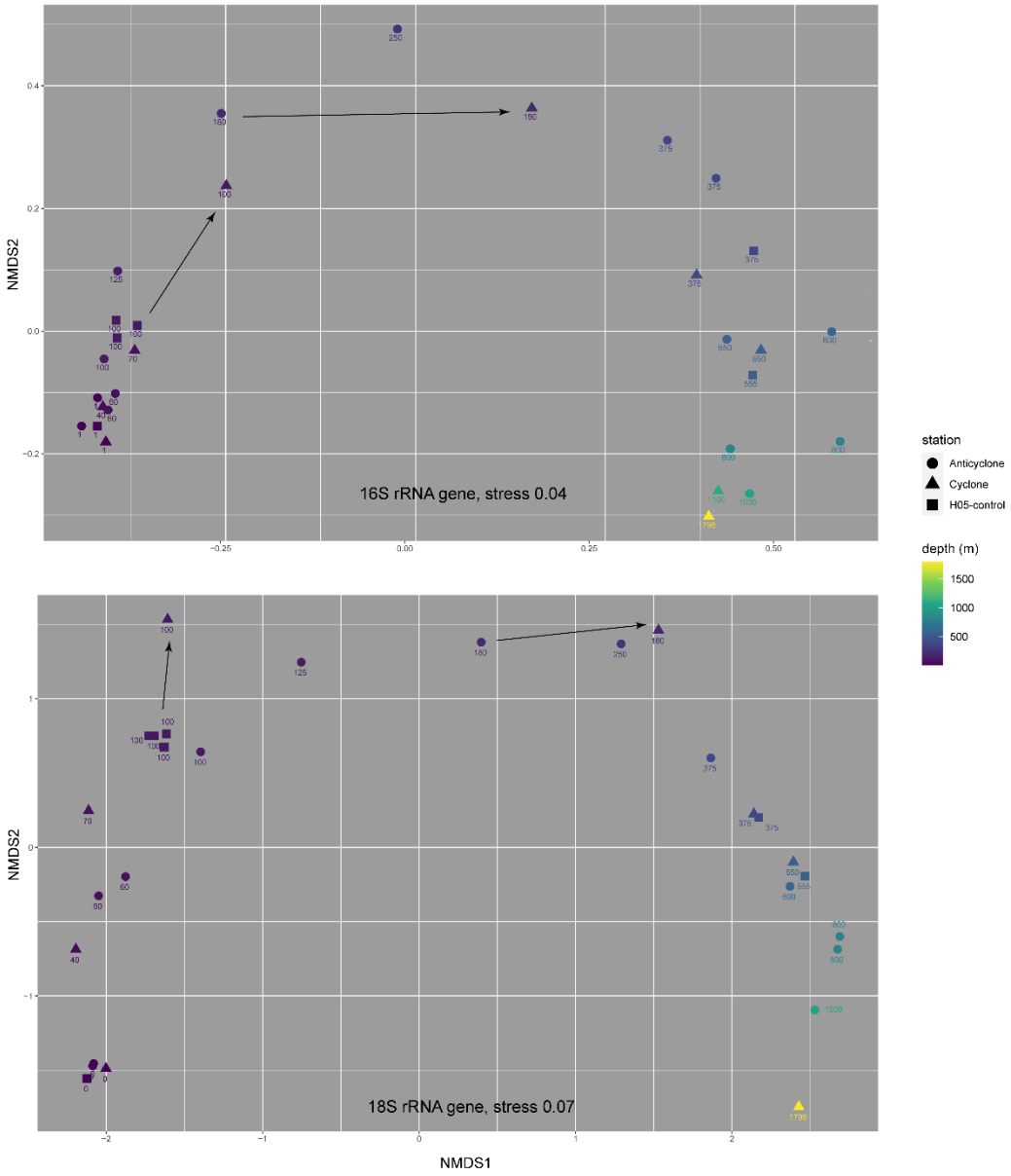

Figure S10. Non-metric multidimensional scaling (NMDS, based on the Bray-Curtis dissimilarity in amplicon sequence variants) plots, showing a potential shift in the composition of bacterioplankton (top) and unicellular planktonic eukaryotes (bottom) communities at the deep chlorophyll maximum and 180 m depths of the cyclonic station, in comparison to the respective depths in the background (H05) and anticyclonic stations. The numbers next to symbols are depth (m).

Table S1 – Results of statistical comparison (one-way ANOVA and Bonferroni-corrected post-hoc t-test, $P<0.05$) between variables (0-180m) at the different stations. The letters represent the different statistical groups. N.A – Not applicable.

Variable	**Background**	**Cyclone**	**Anti-cyclone**
NOx (mmol m^{-2})	B	A	C
PO_4 (mmol m^{-2})	A	A	B
$Si(OH)_4$ (mmol m^{-2})	A	B	A
Chl-*a* (mg m^{-2})	A	A	B
Synechococcus (x10^{10} cells m^{-2})	A	C	B
Prochlorococcus (x10^{10} cells m^{-2})	B	A	C
Pico-eukaryotes (x10^{10} cells m^{-2})	A	B	A
Nano-eukaryotes (x10^{10} cells m^{-2})	A	B	A
Total pico/nano-phytoplankton biomass (mg m^{-2})	B	C	A
Heterotrophic bacteria (x10^{10} cells m^{-2})	A	B	C
Heterotrophic bacteria biomass (mg m^{-2})	A	B	C
Zooplankton (mg m^{-2})	N.A	N.A	N.A
Zooplankton / total phytoplankton biomass	N.A	N.A	N.A
PP (gC m^{-2} d^{-1})	B	A	B
AN – PP/Chl.*a* (gC gChl.a^{-1} day^{-1})	B	A	B
BP (gC m^{-2} d^{-1})	A	B	A
BP/BA (x10^{14} gC $cell^{-1}$ day^{-1})	B	C	A
BP/PP	A	B	A

References

Ben-Ezra T, Krom MD, Tsemel A, Berman-Frank I, Herut B, Lehahn Y, Rahav E, Reich T, Thingstad TF, Sher D (2021) Deep-Sea Research Part I Seasonal nutrient dynamics in the P depleted Eastern Mediterranean Sea. Deep Res Part I 176:103607

Reich T, Ben-Ezra T, Belkin N, TsemelA, Aharonovich D, Roth-Rosenberg D, Givati S, Bialik O, Herut B, Berman-Frank I, Frada M, Krom MD, Lehahn Y, Rahav E and Sher D. (2022). A year in the life of the Eastern Mediterranean Sea: Monthly dynamics of phytoplankton and bacterioplankton in an ultra-oligotrophic sea. Deep Sea Research I, 182 (2022) 103720. https://doi.org/10.1016/j.dsr.2022.103720.